Published in final edited form as:
J Immunol. 2015 January 1; 194(1): 125–133. doi:10.4049/jimmunol.1401644.

OX40- and CD27-mediated co-stimulation synergize with anti-PD-L1 blockade by forcing exhausted CD8+ T cells to exit quiescence

Sarah Buchan[#*], **Teresa Manzo**[#†], **Barry Flutter**[#†], **Anne Rogel**[*], **Noha Edwards**[†], **Lei Zhang**[†], **Shivajanani Sivakumaran**[†], **Sara Ghorashian**[†], **Ben Carpenter**[†], **Clare Bennett**[†], **Gordon J. Freeman**[‡], **Megan Sykes**[§], **Michael Croft**[¶], **Aymen Al-Shamkhani**[*], and **Ronjon Chakraverty**[†]

[*]Cancer Sciences Unit, Faculty of Medicine, University of Southampton

[†]Transplantation Immunology Group, Cancer Institute and Institute for Immunity and Transplantation, University College London

[‡]Department of Medical Oncology, Dana-Farber Cancer Institute, Harvard Medical School

[§]Columbia Center for Translational Immunology, Columbia University Medical Center, New York

[¶]Institute of Allergy and Immunology, La Jolla.

[#] These authors contributed equally to this work.

Abstract

Exhaustion of chronically stimulated CD8$^+$ T cells is a significant obstacle to immune control of chronic infections or tumors. Although co-inhibitory checkpoint blockade with anti-programmed death-ligand 1 (PD-L1) antibody can restore functions to exhausted T cell populations, recovery is often incomplete and dependent upon the pool size of a quiescent T-bet^{high} subset that express lower levels of PD-1. In a model where unhelped, HY-specific CD8$^+$ T cells gradually lose function following transfer to male BMT recipients, we have explored the effect of shifting the balance away from co-inhibition and toward co-stimulation by combining anti-PD-L1 with agonistic antibodies to the tumor-necrosis factor receptor superfamily members, OX40 and CD27. Several weeks following T cell transfer, both agonistic antibodies but especially anti-CD27 demonstrated synergy with anti-PD-L1 by enhancing CD8$^+$ T cell proliferation and effector cytokine generation. Anti-CD27 and anti-PD-L1 synergised by downregulating the expression of multiple quiescence-related genes concomitant with a reduced frequency of T-bet^{high} cells within the exhausted population. However, in the presence of persistent antigen, the CD8$^+$ T cell response was not sustained and the overall size of the effector cytokine-producing pool eventually contracted to levels below that of controls. Thus, CD27-mediated co-stimulation can synergize with co-inhibitory checkpoint blockade to switch off molecular programs for quiescence in

Corresponding Author: Ronjon Chakraverty, Transplantation Immunology Group, Department of Haematology, University College London Phone: +44 207 317 7513 Fax: +44 207 830 2092 r.chakraverty@ucl.ac.uk.

AA-S and RC are joint senior authors

GJF has patents and receives patent royalties on the PD-1 pathway. The other authors declare that they have no conflicts of interest

exhausted T cell populations but at the expense of losing precursor cells required to maintain a response.

Introduction

$CD8^+$ T cell exhaustion resulting from excessive or chronic T-cell receptor (TCR) stimulation poses a significant barrier to the immune control of chronic infections or tumors (1). In the exhausted state, tumor or viral antigen-specific $CD8^+$ T cells become subject to multiple co-inhibitory signals, for example via the programmed death (PD)-1 receptor, and lose functions in step-wise fashion (2). Antibody-mediated blockade of single or multiple co-inhibitory receptors can lead to restoration of $CD8^+$ T cell functions. Indeed, early phase clinical trials of antibody-mediated blockade of the PD-1 pathway have already demonstrated significant efficacy in treating several tumor types (3) and there is now interest in combining this approach with other therapies to maximize the reversal of T cell exhaustion. When analysed at a whole population level, exhausted $CD8^+$ T cells lack gene signatures associated with quiescence and possess disordered expression of gene networks that regulate T cell functions (4). Responsiveness to PD-1 checkpoint blockade however depends upon a relatively quiescent sub-population of PD-1^{low} $CD8^+$ T cells maintained by the T-box transcription factor, T-bet, that retains the capacity to respond to antigen (5). In response to persistent antigen, proliferation of PD-1^{int}T-bet^{high} precursors gives rise to PD-1^{high} T-bet^{low} terminally differentiated progeny that express high levels of another T-box family member, Eomesodermin (5). Thus, the effect of co-inhibitory blockade upon the overall composition of the exhausted repertoire, including the potential deleterious effects of driving terminal differentiation and replicative senescence in antigen-specific T cells requires further study.

In addition to initial TCR activation, productive T cell immunity requires co-stimulation. Members of the tumor-necrosis factor receptor (TNFR) superfamily, including 4-1BB, OX40 and CD27 are important co-stimulatory receptors (reviewed in (6)). Individual or combinatorial co-stimulatory signals via TNFR superfamily members have key roles in maximizing clonal expansion, effector differentiation and survival of T cells (7, 8). For example, OX40 and CD27 co-stimulation trigger the assembly of intracellular signalosomes that induce sustained NF-κB activation and lead to upregulation of pro-survival pathways in T cells (9, 10). Indeed, CD27- and OX40-mediated survival of activated $CD8^+$ T cells may be important in dictating the eventual size of the memory pool following contraction of the primary response (11-15). Where poorly immunogenic tumors or weakly replicating viruses fail to activate TNFR family receptors, enforcing co-stimulation experimentally through application of ligand fusion proteins or agonist antibodies has shown the potential to enhance both primary and recall immunity (6).

The extent to which additional co-stimulation mediated via TNFR family receptors is beneficial under conditions favoring exhaustive differentiation of T cells is less clear. In murine models of chronic lymphocytic choriomeningitis (LCMV) infection, physiological expression of OX40 by virus-specific $CD8^+$ T cells improves viral control (16). On the other hand, continuous signalling via CD27 is implicated in driving even more profound

exhaustion of virus-specific effectors (17). Agonistic antibody-mediated co-stimulation via 4-1BB can be detrimental or beneficial in promoting control of chronic LCMV according to the precise treatment schedule (18). Thus, where expression of co-stimulatory ligands is already elevated or plentiful, driving further co-stimulation may have limited value. However, exhaustive $CD8^+$ T cell differentiation may also occur under conditions where co-stimulatory ligand expression is low, for example within tumors (19) or at late time points following allogeneic stem cell transplantation (20). In the absence of help, non-licensed antigen-presenting cells may lack the repertoire of co-stimulatory ligands required for full generation of productive immunity; in this context, co-inhibitory signals could supervene earlier and accelerate failure of chronically stimulated $CD8^+$ T cells.

In this study, we have tested the hypothesis that provision of additional co-stimulation via TNFR-family receptors under non-inflammatory conditions will aid restoration of functions to exhausted $CD8^+$ T cells. We find that agonistic antibodies to OX40 and especially to CD27 synergize with anti-PD-L1 by enhancing proliferation and effector cytokine generation. CD27-mediated co-stimulation synergized with co-inhibitory checkpoint blockade to switch off molecular programs for quiescence in exhausted T cell populations but this occurred at the expense of losing precursor cells required to maintain the response.

Materials and Methods

Animals

Female C57BL/6 (B6) and B6.SJL (CD45.1) mice were purchased from the Frederick Cancer Research facility and bred in house. MataHari (Mh) TCR transgenic mice on a B6.PL-Thya/Cy background were obtained from Dr. Julian Dyson, Imperial College London (21). *Ox40* −/− mice were provided by Michael Croft and bred in house (22). All procedures were approved by local institutional research committees and conducted in accordance with NIH or United Kingdom Home Office Animals (Scientific Procedures) Act of 1986.

Programmed Death-Ligand 1(PD-L1), OX40, OX40L and CD27 antibodies

Anti-mouse PD-L1 (10F.9G2), anti-OX40 (OX86), anti-CD27 (AT124-1) and their respective isotype controls have been described previously (23-26).

BMT and adoptive T cell transfer

Male B6 mice received 9Gy irradiation followed by receipt of 5×10^6 female B6 bone marrow cells. Seven days later, 1×10^6 Mh $CD8^+$ transgenic T cells with or without additional 2.5×10^6 female B6 polyclonal CD4+ T cells were transferred to BMT recipients (20). Individual $CD4^+$ and $CD8^+$ donor populations were selected using CD4/CD8 T cell isolation kits (Miltenyi Biotec). Uptake of BrdU was used to examine the turnover of cells *in vivo* at later time points by administration of 0.8 mg/ml BrdU (Sigma, UK) in the water of recipient mice over 7 days prior to analysis.

Antibodies and flow cytometry

The following cell surface antibodies (purchased from eBioscience, San Diego, CA) and their respective isotype controls were used: anti-CD8α (53-6.7), anti-CD27 (LG.7F9), anti-CD45.1 (A20), anti-CD45.2 (104), anti-CD107a (1D4B), anti-Thy1.1 (HIS51) anti-PD-1 (J43) and anti-OX40 (OX86). Anti-Vβ8.3 TCR (1B3.3) was purchased from BD Biosciences (Oxford, UK). Direct intracellular staining was carried out using anti-perforin (OMAK-D), anti-T-bet (4B10) and anti-Eomes (Dan11mag) and isotype controls, purchased from eBioscience, San Diego, CA or anti-granzyme B (GRB05) from Life Technologies, UK. Following brief peptide re-stimulation, intracellular staining was performed using anti-IFN-γ (XMG1.2) or anti-TNF-α (MP6-XT22) together with the appropriate isotype controls (BD Biosciences, Oxford, UK). Intra-nuclear staining for BrdU was carried out using anti-BrdU-APC flow kit (BD Biosciences, Oxford, UK), according to the manufacturer's instructions. To detect CD107a cells were restimulated for 4 hours in the presence or absence of 1μM UTY peptide with Golgi-Stop (BD Pharmingen) in the presence of anti-CD107a or isotype control. Cells were then re-surface stained with anti-CD107a or isotype. Flow cytometric analysis was performed on a LSRFortessa or FACs Canto II (BD Biosciences) and cell counting performed on a Coulter Counter (Beckman Coulter).

Intracellular cytokine staining

Cells from spleen or blood were analyzed for antigen-specific IFN-γ or TNFα release by *ex vivo* intracellular staining. Briefly, cells were cultured in the absence or in the presence of 1μM of the peptide UTY (WMHHNMDLI) or irrelevant peptide (OVA SIINFEKL) for 4h (ProImmune or Peptide Protein Research, UK) and Brefeldin A (GolgiPlug, BD Pharmingen) was added either at the start or for the last 2h. Cells were then surface stained for CD8 and Vβ8.3, or relevant congenic markers, fixed and permeabilized and then analyzed for intracellular cytokine staining by addition of the appropriate antibody.

Gene expression analysis

mRNA was isolated using the RNeasy Micro Kit followed by cDNA generation using the RT^2 PreAMP cDNA Synthesis Kit (both QIAGEN). Gene expression analysis was performed using the RT^2 Profiler T cell Anergy and Immune Tolerance PCR Array by quantitative PCR using *Actb*, *Gusb* and *Hsp90ab1* housekeeping genes for normalisation (Qiagen). Raw threshold data generated by PCR was uploaded to a dedicated web portal for further analysis (http://www.sabiosciences.com/pcrarraydataanalysis.php).

Statistical analyses

Statistical analyses were performed using the unpaired t-test (two tailed). A p value < 0.05 was considered to be significant (*$p<0.05$, **$p<0.01$, ***$p<0.001$).

Results

Agonistic co-stimulation via OX40 synergizes with anti-PD-L1 to recover functions of helpless, exhausted CD8$^+$ T cells

We have shown previously that TCR-transgenic MataHari (Mh) CD8$^+$ T cells (specific for the male antigen, UTY) become exhausted following delayed transfer to male, MHC-matched BMT recipients (20). Administration of anti-PD-L1 can partially rescue the functions of exhausted Mh CD8$^+$ T cells under conditions where they are co-transfered with polyclonal female CD4+ T cells (20). Because CD4$^+$ T cells can protect against exhaustion in models of chronic viral infection (27), we first evaluated whether exhaustion of helpless Mh CD8$^+$ T cells could similarly be reversed following anti-PD-L1. As shown in Figure 1A, both CD4 helped and unhelped Mh CD8$^+$ T cells (Thy1.1+ Vβ8.3+) demonstrated similar reductions in their capacity to produce IFN-γ over time following their transfer to male B6 BMT recipients. However, Mh CD8$^+$ T cell expression of PD-1 was higher in the unhelped versus the helped experimental group (Figure 1B) and although anti-PD-L1 treatment could enhance proliferation from baseline in helpless Mh CD8$^+$ T cells, it had little effect upon generation of IFN-γ (Figure 1C). This was in contrast to helped conditions, where as we have previously reported (20), anti-PD-L1 treatment increased both proliferation and IFN-γ generation. Because the amount of male antigen remains constant throughout the experiment, these data show that CD4$^+$ T cells can protect CD8$^+$ T cells from exhaustion through effects that are independent of any change in overall antigen load.

In initial experiments to examine the effect of additional co-stimulation upon rescue of exhausted Mh CD8$^+$ T cells, we first evaluated the expression of TNFR family members that are up-regulated in response to TCR activation (OX40, 4-1BB). Compared to naive input cells, we observed increased expression of OX40 which was equivalent upon both helped and unhelped CD8$^+$ T cells at day 42 following transfer (Figure 2A). To test the effect of enforcing OX40 co-stimulation in helped compared to unhelped Mh CD8$^+$ T cells, we administered an agonist anti-OX40 monoclonal antibody (OX86) on day 35 following T cell transfer, alone or in combination with anti-PD-L1 given on days 36 and 39, and evaluated the response at day 42. Under both helped and unhelped conditions, anti-OX40 given alone had no effect upon proliferation (as estimated by BrdU incorporation) or IFN-γ production by Mh CD8$^+$ T cells (Figure 2B, C and Supplementary Figure S1A). However, when anti-OX40 was combined with anti-PD-L1 blockade, we observed synergistic increases in Mh CD8$^+$ T cell proliferation that were evident in helpless but not helped cells (Figure 2B, C). In the helpless setting, the combination of anti-PD-L1 and anti-OX40 also synergised to increase the absolute numbers of IFN-γ+ Mh CD8$^+$ T cells in the spleen although these effects were relatively modest when evaluated on a per-cell basis (Figure 2B, C and Figure S1A). The synergy for effector cytokine expression in the combined treatment group was limited to IFN-γ; anti-OX40 alone had no effect upon TNF-α generation, whereas anti-PD-L1 induced a minor increase from baseline with no further increase upon the addition of anti-OX40 (Supplementary Figure S1B). No increases were observed in the frequency of Mh CD8$^+$ T cells dual staining for IFN-γ and TNF-α in any treatment group (Figure S1B). Because OX40 is expressed constitutively on murine Treg and is inducible on other cells including NK and NKT cells (7), we also tested whether the effect of combined anti-PD-L1

and anti-OX40 would still occur under conditions where Mh $CD8^+$ T cells expressed OX40 but other immune cell populations did not. Thus, we transferred unhelped Mh $CD8^+$ T cells to male BMT recipients as set out in Figure 2B, but reconstituted irradiated male recipients with female OX40−/− BM. Under these experimental conditions, anti-PD-L1 treatment alone had no effect whereas anti-OX40 and anti-PD-L1 induced significant increases in absolute numbers of IFN-γ+ Mh $CD8^+$ T cells, indicating an intrinsic effect of co-stimulation upon the transferred $CD8^+$ T cell population (Supplementary Figure S1C).

Agonistic co-stimulation via CD27 is more effective than OX40 in the initial reversal of $CD8^+$ T cell exhaustion

CD27 is another TNFR family member that differs from OX40 in that its expression is constitutive upon naive $CD8^+$ T cells. As shown in Figure 3A, CD27 was expressed to a similar extent upon both input naive and unhelped exhausted Mh $CD8^+$ T cells at day 42 (Figure 3A). In a similar approach to the experiments outlined in Figure 2, we applied agonistic anti-CD27 alone or in combination with anti-PD-L1 to male BMT recipients adoptively transferred with unhelped Mh $CD8^+$ T cells five weeks earlier. In contrast to anti-OX40, we found that anti-CD27 given alone significantly improved proliferation of unhelped Mh $CD8^+$ T cells although it had no effect upon IFN-γ generation (Figure 3B, C and Figure S1). When anti-CD27 was combined with anti-PD-L1, additive effects upon proliferation and synergistic increases in IFN-γ expression were noted (Figure 3B, C and Figure S1A). The synergy for effector cytokine expression in the combined treatment group was limited to IFN-γ; both anti-CD27 and anti-PD-L1 alone induced minor increases in TNF-α generation, with no further increases in the combined treatment group (Figure S1B). No increases were observed in the frequency of Mh $CD8^+$ T cells dual staining for IFN-γ and TNF-α in any treatment group (Figure S1B). Similar to our findings with anti-OX40 and anti-PD-L1, synergy between anti-CD27 and anti-PD-L1 was only observed under helpless conditions (Supplementary Figure S1D). To compare the effects of combining anti-PD-L1 with each TNFR antibody, we performed direct comparisons of anti-OX40 or anti-CD27 in combination with anti-PD-L1. As shown in Figure 4, anti-CD27 and anti-OX40 in combination with anti-PD-L1 were similarly effective in promoting a proliferative response in Mh $CD8^+$ T cells and in enhancing effector function as evaluated by CD107a expression. However, anti-PD-L1 plus anti-CD27 were more effective than anti-PD-L1 and anti-OX40 in enhancing the effector function of Mh $CD8^+$ T cells as evaluated by IFN-γ upon peptide stimulation (Figure 4).

Molecular profiling of T cell responses to TNFR co-stimulation in the presence or absence of co-inhibitory checkpoint blockade

In order to identify potential mechanisms underlying the synergy between OX40 and CD27 agonistic antibodies and anti-PD-L1, we extracted mRNA from flow sorted Mh $CD8^+$ T cells derived from mice, 7 days following the commencement of individual or combined antibody combinations (day 42, n=4 mice/group) and then performed quantitative RT-PCR for 84 individual genes linked to T cell tolerance and effector functions. As shown in the heat map in Figure 5A, the gene expression profiles of Mh $CD8^+$ T cells derived from mice receiving anti-CD27 and anti-PD-L1 segregated from the other groups although there was some overlap, primarily with the anti-CD27 group and the combined anti-OX40/anti-PD-L1

group. Within the subset of genes showing reduced transcription in the anti-CD27 and anti-PD-L1 group, we found that a significant number were involved in quiescence and/or anergy, including genes encoding transcriptional repressors (*Foxp1, Foxp3, Egr2, Egr3, Ing4*), E3 ubiquitin ligases (*Itch, Rnf128*) and other genes encoding proteins preventing TCR-proximal signaling (*Dgka, Dgkz*) or providing coinhibitory signals (*Ctla4, Pdcd1, Btla).* Using a >2.0 fold reduction cut-off, we evaluated how these genes were affected in each of the experimental groups (Figure 5B). All the treatment groups were characterized by a core signature of reduced *Egr3* expression and with the exception of the anti-PD-L1 group, reduced *Foxp3* expression. *Egr2*, an *Egr3*-related transcription factor gene required for the induction of several other anergic factors (28-30) was reduced in the anti-CD27 group and both the combined treatment groups. In addition, the combined anti-CD27 and anti-PD-L1 group showed reductions in the expression of a more extensive set of anergy-related genes (Figure 5B). The number of down-regulated genes was not as wide in the combined anti-OX40 and anti-PD-L1 group despite the demonstration of significant synergy in terms of proliferation; however, this group was additionally characterized by reduced expression of the co-inhibitory receptor *Btla* (an effect that was also seen but to a lesser extent in the anti-OX40 group, Figure 5B and data not shown). To evaluate this gene expression pattern in more detail, we examined the expression of a panel of 10 genes that have been shown individually to be necessary for anergy or quiescence (28-30). When anti-CD27 was combined with anti-PD-L1, the entire panel of anergy and quiescence genes showed reduced expression with a clear synergistic pattern. In the combined anti-OX40 and anti-PD-L1 group, marked synergy was observed for *Egr2* down-regulation with further additive effects upon *Rnf128* repression. In contrast, with the exception of *Egr3*, none of the anergy genes was down-regulated in the PD-L1 group. We also extended this analysis to evaluate the entire gene set using a >2.0 fold change cut-off (Supplementary Figure S2). Using these criteria, it was noteworthy that the changes in the anergy- and quiescence-related genes were not paralleled by reciprocal increases in the expression of genes encoding effector molecules or the transcriptional regulators that induce them when considered at a whole population level. Indeed, the expression of several regulator genes required for effector differentiation (*Jak3, Gata3, Stat6, Tbx21, Icos, Irf4, Fos, Jun*) were in fact reduced in Mh $CD8^+$ T cells derived from mice receiving anti-CD27 and anti-PD-L1.

Loss of T-bet^{high}Eomes^{low} cells by combined treatment with anti-CD27 and anti-PD-L1 leads to eventual contraction of the effector pool

In the model of $CD8^+$ T cell exhaustion following chronic LCMV infection, a quiescent T-bet^{high}Eomes^{low}PD-1^{low} precursor population is required for maintaining residual immunity to antigen and for restoration of functions in response to PD-1 checkpoint blockade (5, 31). Because anti-CD27 alone, and in combination with anti-PD-L1, switched off a number of anergy- or quiescence-related genes, we wanted to determine how this would impact upon the precusor population and maintenance of immunity long-term. We therefore conducted experiments in which we tracked Mh $CD8^+$ T cell function in relation to T-bet and Eomes expression at both early and late time points following antibody treatment. Using the same treatment schedule as Figure 3, but starting antibody treatment at day 59 following unhelped T cell transfer, we again observed a synergistic increase in the frequency and absolute numbers of peripheral blood Mh $CD8^+$ T cells in the combined anti-CD27 and anti-PD-L1

group (Figure 6A-B). As in previous experiments, the combined antibody treatment led to a synergistic increase in the frequency of IFN-γ^+ cells upon peptide re-stimulation on day 65 with a similar trend for absolute numbers (Figure 6B). We then evaluated early changes in T-bet and Eomes expression in the responding Mh $CD8^+$ T cell populations from each group. In the control group, peripheral blood Mh $CD8^+$ T cells were heterogeneous with respect to T-box transcription factor expression, retaining a significant pool of T-$bet^{high}Eomes^{low}$ precursor-like cells that constituted ~40% of the entire population and a smaller, terminally differentiated T-$bet^{low}Eomes^{high}$ subset of about ~10% (Figure 6C). Although there were no differences in the surface expression of CD27 in T-bet^{high} versus T-bet^{low} cells (data not shown), we reasoned that anti-CD27 would primarily target the former population because of its greater replicative potential (5). Indeed, anti-PD-L1 and anti-CD27 treatment induced a rapid reduction in the frequency of T-$bet^{high}Eomes^{low}$ Mh $CD8^+$ T cells and as predicted by their precursor-product relationship (5), this was linked to a reciprocal increase in the frequency of T-$bet^{low}Eomes^{high}$ cells; intermediate changes as compared to the controls were observed in the single anti-CD27 or anti-PD-L1 groups (Figure 6C).

In spleens from control mice, we observed a decline over time in the relative frequency of Mh $CD8^+$ T cells that were T-$bet^{high}Eomes^{low}$ versus T-$bet^{low}Eomes^{high}$, consistent with ongoing antigen activation and terminal differentiation (Supplementary Figure S3). To determine the long-term effects of anti-CD27 and/or anti-PD-L1 upon Mh $CD8^+$ T cell function and the balance between precursor versus terminally-differentiated subsets, we re-evaluated IFN-γ synthesis and T-bet/Eomes expression in recipient spleens at day 120 after T cell transfer,61 days following anti-CD27 and/or anti-PD-L1 administration (Figure 6D-F). Despite the initial rescue of the response following combined treatment, the frequency of Mh $CD8^+$ T cells capable of producing IFN-γ at day 120 in response to relevant peptide was further reduced compared to the control (2.5-fold) or singly-treated anti-PD-L1 group (4-fold) (Figure 6D). The absolute number of total and IFN-γ+ Mh $CD8^+$ T cells/spleen were also significantly lower in the combined anti-CD27/anti-PD-L1 group compared with the control (2-fold) and anti-PD-L1 group (17-fold) (Figure 6D and data not shown); indeed, we noted similar reductions in the pool size of functional Mh $CD8^+$ T cells within the single anti-CD27 antibody group. In contrast, the absolute numbers of IFN-γ+ Mh $CD8^+$ T cells/spleen in the single anti-PD-L1 antibody-treated mice were greater than controls indicating a long-term protective effect of this antibody against exhaustion. To determine how spleen Mh $CD8^+$ T cell function at day 120 correlated with expression of T-bet and Eomes, we performed intracellular staining for each transcription factor. Consistent with the hypothesis that anti-CD27 was driving further loss of precursors required for maintaining antigen responsiveness, the surviving Mh $CD8^+$ T cells in both the combined anti-CD27 and anti-PD-L1 group and the single anti-CD27 group showed significant skewing to a terminally-differentiated T-$bet^{low}Eomes^{high}$ phenotype with a relative loss of cells that were T-$bet^{high}Eomes^{low}$ (Figure 6E). Furthermore, in a pooled analysis of all the groups, we observed a significant negative correlation between the percentage of cells that were $Eomes^{high}$ and the perecntage of cells capable of generating IFN-γ (Figure 6F). Thus, additional CD27 co-stimulation enables temporary rescue of exhausted $CD8^+$ T cells but at the expense of driving their terminal differentiation and eventual loss of function.

Discussion

In this study, we have shown that anti-OX40- and anti-CD27-mediated co-stimulation synergized with co-inhibitory checkpoint blockade to restore functions of exhausted, helpless $CD8^+$ T cells. When combined with anti-PD-L1, stimulation of T cells through OX40 and especially CD27 primarily acted to block molecular programs for anergy or quiescence, driving $CD8^+$ T cells to undergo rapid proliferation and terminal differentiation. However, transient improvements in effector functions occurred at the expense of loss of precursor cell populations capable of sustaining the response.

As in models of chronic viral infection, unhelped HY-specific $CD8^+$ T cells become more exhausted than helped cells and less amenable to rescue through anti-PD-L1 blockade alone. These findings are also consistent with the concept that $CD4^+$ T cells are less prone to exhaustive differentiation than $CD8^+$ T cells (32) and thus, capable of providing helper signals at the priming and/or maintenance phase of the response (27). Because the amount of male antigen is 'fixed' during the development of HY-specific $CD8^+$ T cell exhaustion following BMT, the capacity of $CD4^+$ T cells to mitigate against $CD8^+$ T cell exhaustion is independent of any effect upon the overall antigen load. Lack of help was linked to higher expression of PD-1 upon the exhausted Mh $CD8^+$ T cell repertoire and this is likely to explain the relative failure of helpless cells to respond to anti-PD-L1. The effect of $CD4^+$ T cells upon PD-1 expression could be direct, for example through the synthesis of IL-2 which can limit upregulation of PD-1 upon $CD8^+$ memory T cells (33) or indirect, through 'licensing' of antigen-presenting cells (34). Lack of $CD4^+$ T cell help is also a major obstacle to successful immunotherapy of cancer (35). In a tumor model characterized by ineffective antigen presentation via MHC Class II (36), we have also observed synergy between anti-OX40 or anti-CD27 with anti-PD-L1. Thus, following vaccination with irradiated B16 melanoma cells expressing Flt3-ligand, addition of either anti-OX40 or anti-CD27 to anti-PD-L1 synergized to enhance tumor infiltration by endogenous T cells and significantly delay tumor growth (SB and AA-S, unpublished data). The finding that tumor-reactive $CD8^+$ T cells within human melanomas frequently co-express PD-1 and TNFR family co-stimulatory molecules (37) suggests that this approach may have clinical application.

OX40- or CD27-mediated co-stimulation activates several pathways downstream of the TCR that are inhibited via PD-1 signaling, including PI3K-Akt, NF-κB and NFAT (38). In addition, PD-1 ligation also interrupts proximal TCR signalling through mechanisms that require recruitment of SHP2 to an ITSM contained within its cytoplasmic domain (39). For the most part, we observed that the interaction between OX40- and especially CD27-induced co-stimulation was synergistic with anti-PD-L1, indicating that TNFR family-mediated signaling was acting on molecular pathways distinct from those inhibited by PD-1. The lack of synergy in the helped setting would also imply that signaling via OX40 or CD27 is somehow suboptimal in unhelped $CD8^+$ T cells, although whether this is a T-cell intrinsic effect and/or the result of reduced ligand expression requires further study. Following co-treatment with anti-CD27 and anti-PD-L1 especially, several genes encoding proteins promoting anergy or quiescence were sharply downregulated. This finding was unexpected because the transcriptional programs that underlie exhaustion and anergy are often viewed

as being distinct (40), with lack of quiescence being a key property assigned to exhausted T cells when the population is examined as a whole (4). Indeed, the behaviour of the Mh $CD8^+$ T cells upon adoptive transfer to male recipients did not parallel *in vivo* models of anergy where T cell functions are impaired almost immediately upon antigen encounter (41). Instead, more akin to models of exhaustion, the functions of Mh $CD8^+$ T cells were progressively lost over time (Supplementary Figure S4). Nevertheless, as the pro-inflammatory effects of irradiation diminish, it is possible that reduced levels of co-stimulation (signal 2) also induce overlapping anergic molecular programs that contribute to the observed T cell dysfunction.

When evaluated at a whole population level, we did not observe reciprocal changes within the anergy and effector gene sets in T cells following combined co-inhibitory blockade and enforced CD27-mediated co-stimulation. Reduced expression of anergy-related factors would be predicted to enhance TCR-proximal signalling leading to downstream activation of Ras, ERK and JNK pathways that in turn induce effector differentiation (29). However, several downstream master regulators of effector gene expression were in fact moderately down-regulated in the combined treatment group when evaluated directly *ex vivo* despite the transiently increased capacity of T cells to undergo degranulation or generation of IFN-γ upon re-stimulation. Without performing single cell analyses of gene expression, we cannot exclude the possibility that the lack of reciprocity reflects the fact that the population evaluated is mixed, including cells that remain exhausted as well as those with restored functions. Alternatively, the Q-PCR may miss the effects of post-transcriptional regulation of the relevant genes.. However, recent studies have also revealed different patterns of connectivity in exhausted compared to effector or memory cells, such that specific transcription factors (e.g. T-bet) can possess highly variable transcriptional interactions according to their cellular context (4). Thus, removal of anergy factors and enhanced TCR-coupled signal transduction may be insufficient to fully restore effector programs that have become disconnected in the setting of continual TCR stimulation.

Although combined anti-CD27 and anti-PD-L1 led to robust increases in proliferation and measurable gains in effector function upon re-stimulation, these effects were not sustained. It is known that tolerant cells induced to undergo proliferation in response to lymphopenia also transiently improve their effector functions but then switch back to their tolerant state as epigenetic changes required for tolerance are re-established (42); it is possible that a similar mechanism applies in the setting of exhaustion. However, an alternative and non-exclusive mechanism suggested in this study is that the loss of quiescence factors induced by anti-CD27 with or without anti-PD-L1 eventually leads to a loss of precursor cells and consequent reductions in the total pool size of antigen-specific T cells as effectors reach their Hayflick limit and undergo replicative senescence (43). The fact that the effector pool was also eventually diminished in the group treated with anti-CD27 antibody alone suggests that reductions in only a subset of anergy factors are sufficient for the loss of T-bet^{high} precursors to occur. Future studies addressing the potential of combined co-inhibitory checkpoint blockade and co-stimulation therapies will therefore need to examine in detail how restoration of exhausted T cell functions affects the composition of the emerging repertoire according to markers of replicative potential such as T-box transcription factor

expression and telomere length. The risk that such therapies deplete the effector pool still further may be greatest when levels of antigen and/or co-stimulation are already high.

Supplementary Material

Refer to Web version on PubMed Central for supplementary material.

Acknowledgements

We thank Hans Stauss for his helpful comments on the manuscript.

Funding: Leukaemia and Lymphoma Research (RC, AAS, SLB); NIH (P01 AI56299 and R01 A1051559, GJF) and NIH/NCI P01 CA111519 (MS)

Abbreviations

BM	Bone marrow
BMT	Bone marrow transplantation
LCMV	Lymphocytic choriomeningitis virus
Mh	MataHari
PD-1	Programmed death 1
PD-L1	Programmed death-ligand 1
TNFR	Tumor-necrosis factor receptor

References

1. Wherry EJ. T cell exhaustion. Nature immunology. 2011; 12:492–499. [PubMed: 21739672]
2. Blackburn SD, Shin H, Haining WN, Zou T, Workman CJ, Polley A, Betts MR, Freeman GJ, Vignali DA, Wherry EJ. Coregulation of CD8+ T cell exhaustion by multiple inhibitory receptors during chronic viral infection. Nat Immunol. 2009; 10:29–37. [PubMed: 19043418]
3. Brahmer JR, Tykodi SS, Chow LQ, Hwu WJ, Topalian SL, Hwu P, Drake CG, Camacho LH, Kauh J, Odunsi K, Pitot HC, Hamid O, Bhatia S, Martins R, Eaton K, Chen S, Salay TM, Alaparthy S, Grosso JF, Korman AJ, Parker SM, Agrawal S, Goldberg SM, Pardoll DM, Gupta A, Wigginton JM. Safety and activity of anti-PD-L1 antibody in patients with advanced cancer. The New England journal of medicine. 2012; 366:2455–2465. [PubMed: 22658128]
4. Doering TA, Crawford A, Angelosanto JM, Paley MA, Ziegler CG, Wherry EJ. Network analysis reveals centrally connected genes and pathways involved in CD8+ T cell exhaustion versus memory. Immunity. 2012; 37:1130–1144. [PubMed: 23159438]
5. Paley MA, Kroy DC, Odorizzi PM, Johnnidis JB, Dolfi DV, Barnett BE, Bikoff EK, Robertson EJ, Lauer GM, Reiner SL, Wherry EJ. Progenitor and terminal subsets of CD8+ T cells cooperate to contain chronic viral infection. Science. 2012; 338:1220–1225. [PubMed: 23197535]
6. Croft M. The role of TNF superfamily members in T-cell function and diseases. Nature reviews. Immunology. 2009; 9:271–285. [PubMed: 19319144]
7. Croft M. Control of immunity by the TNFR-related molecule OX40 (CD134). Annual review of immunology. 2010; 28:57–78.
8. Redmond WL, Ruby CE, Weinberg AD. The role of OX40-mediated co-stimulation in T-cell activation and survival. Crit Rev Immunol. 2009; 29:187–201. [PubMed: 19538134]
9. Song J, So T, Cheng M, Tang X, Croft M. Sustained survivin expression from OX40 costimulatory signals drives T cell clonal expansion. Immunity. 2005; 22:621–631. [PubMed: 15894279]

10. Song J, So T, Croft M. Activation of NF-kappaB1 by OX40 contributes to antigen-driven T cell expansion and survival. Journal of immunology. 2008; 180:7240–7248.
11. Hendriks J, Xiao Y, Borst J. CD27 promotes survival of activated T cells and complements CD28 in generation and establishment of the effector T cell pool. The Journal of experimental medicine. 2003; 198:1369–1380. [PubMed: 14581610]
12. Mousavi SF, Soroosh P, Takahashi T, Yoshikai Y, Shen H, Lefrancois L, Borst J, Sugamura K, Ishii N. OX40 costimulatory signals potentiate the memory commitment of effector CD8+ T cells. Journal of immunology. 2008; 181:5990–6001.
13. Peperzak V, Xiao Y, Veraar EA, Borst J. CD27 sustains survival of CTLs in virus-infected nonlymphoid tissue in mice by inducing autocrine IL-2 production. The Journal of clinical investigation. 2010; 120:168–178. [PubMed: 19955658]
14. Taraban VY, Rowley TF, Al-Shamkhani A. Cutting edge: a critical role for CD70 in CD8 T cell priming by CD40-licensed APCs. Journal of immunology. 2004; 173:6542–6546.
15. Welten SP, Redeker A, Franken KL, Benedict CA, Yagita H, Wensveen FM, Borst J, Melief CJ, van Lier RA, van Gisbergen KP, Arens R. CD27-CD70 costimulation controls T cell immunity during acute and persistent cytomegalovirus infection. J Virol. 2013; 87:6851–6865. [PubMed: 23576505]
16. Boettler T, Moeckel F, Cheng Y, Heeg M, Salek-Ardakani S, Crotty S, Croft M, von Herrath MG. OX40 facilitates control of a persistent virus infection. PLoS pathogens. 2012; 8:e1002913. [PubMed: 22969431]
17. Penaloza-MacMaster P, Ur Rasheed A, Iyer SS, Yagita H, Blazar BR, Ahmed R. Opposing effects of CD70 costimulation during acute and chronic lymphocytic choriomeningitis virus infection of mice. J Virol. 2011; 85:6168–6174. [PubMed: 21507976]
18. Vezys V, Penaloza-MacMaster P, Barber DL, Ha SJ, Konieczny B, Freeman GJ, Mittler RS, Ahmed R. 4-1BB signaling synergizes with programmed death ligand 1 blockade to augment CD8 T cell responses during chronic viral infection. Journal of immunology. 2011; 187:1634–1642.
19. Baitsch L, Baumgaertner P, Devevre E, Raghav SK, Legat A, Barba L, Wieckowski S, Bouzourene H, Deplancke B, Romero P, Rufer N, Speiser DE. Exhaustion of tumor-specific CD8(+) T cells in metastases from melanoma patients. The Journal of clinical investigation. 2011; 121:2350–2360. [PubMed: 21555851]
20. Flutter B, Edwards N, Fallah-Arani F, Henderson S, Chai JG, Sivakumaran S, Ghorashian S, Bennett CL, Freeman GJ, Sykes M, Chakraverty R. Nonhematopoietic antigen blocks memory programming of alloreactive CD8+ T cells and drives their eventual exhaustion in mouse models of bone marrow transplantation. The Journal of clinical investigation. 2010; 120:3855–3868. [PubMed: 20978352]
21. Valujskikh A, Lantz O, Celli S, Matzinger P, Heeger PS. Cross-primed CD8(+) T cells mediate graft rejection via a distinct effector pathway. Nat Immunol. 2002; 3:844–851. [PubMed: 12172545]
22. Rogers PR, Song J, Gramaglia I, Killeen N, Croft M. OX40 promotes Bcl-xL and Bcl-2 expression and is essential for long-term survival of CD4 T cells. Immunity. 2001; 15:445–455. [PubMed: 11567634]
23. al-Shamkhani A, Birkeland ML, Puklavec M, Brown MH, James W, Barclay AN. OX40 is differentially expressed on activated rat and mouse T cells and is the sole receptor for the OX40 ligand. Eur J Immunol. 1996; 26:1695–1699. [PubMed: 8765008]
24. French RR, Taraban VY, Crowther GR, Rowley TF, Gray JC, Johnson PW, Tutt AL, Al-Shamkhani A, Glennie MJ. Eradication of lymphoma by CD8 T cells following anti-CD40 monoclonal antibody therapy is critically dependent on CD27 costimulation. Blood. 2007; 109:4810–4815. [PubMed: 17311995]
25. Malmstrom V, Shipton D, Singh B, Al-Shamkhani A, Puklavec MJ, Barclay AN, Powrie F. CD134L expression on dendritic cells in the mesenteric lymph nodes drives colitis in T cell-restored SCID mice. Journal of immunology. 2001; 166:6972–6981.
26. Rodig N, Ryan T, Allen JA, Pang H, Grabie N, Chernova T, Greenfield EA, Liang SC, Sharpe AH, Lichtman AH, Freeman GJ. Endothelial expression of PD-L1 and PD-L2 down-regulates CD8+ T cell activation and cytolysis. Eur J Immunol. 2003; 33:3117–3126. [PubMed: 14579280]

27. Elsaesser H, Sauer K, Brooks DG. IL-21 is required to control chronic viral infection. Science. 2009; 324:1569–1572. [PubMed: 19423777]
28. Parish IA, Rao S, Smyth GK, Juelich T, Denyer GS, Davey GM, Strasser A, Heath WR. The molecular signature of CD8+ T cells undergoing deletional tolerance. Blood. 2009
29. Wells AD. New insights into the molecular basis of T cell anergy: anergy factors, avoidance sensors, and epigenetic imprinting. Journal of immunology. 2009; 182:7331–7341.
30. Zheng Y, Zha Y, Gajewski TF. Molecular regulation of T-cell anergy. EMBO Rep. 2008; 9:50–55. [PubMed: 18174897]
31. Blackburn SD, Shin H, Freeman GJ, Wherry EJ. Selective expansion of a subset of exhausted CD8 T cells by alphaPD-L1 blockade. Proc Natl Acad Sci U S A. 2008; 105:15016–15021. [PubMed: 18809920]
32. Swain SL, McKinstry KK, Strutt TM. Expanding roles for CD4(+) T cells in immunity to viruses. Nature reviews. Immunology. 2012; 12:136–148.
33. Fuse S, Tsai CY, Molloy MJ, Allie SR, Zhang W, Yagita H, Usherwood EJ. Recall responses by helpless memory CD8+ T cells are restricted by the up-regulation of PD-1. Journal of immunology. 2009; 182:4244–4254.
34. Isogawa M, Chung J, Murata Y, Kakimi K, Chisari FV. CD40 activation rescues antiviral CD8+ T cells from PD-1-mediated exhaustion. PLoS pathogens. 2013; 9:e1003490. [PubMed: 23853599]
35. Kennedy R, Celis E. Multiple roles for CD4+ T cells in anti-tumor immune responses. Immunological reviews. 2008; 222:129–144. [PubMed: 18363998]
36. Gerner MY, Casey KA, Mescher MF. Defective MHC class II presentation by dendritic cells limits CD4 T cell help for antitumor CD8 T cell responses. Journal of immunology. 2008; 181:155–164.
37. Gros A, Robbins PF, Yao X, Li YF, Turcotte S, Tran E, Wunderlich JR, Mixon A, Farid S, Dudley ME, Hanada K, Almeida JR, Darko S, Douek DC, Yang JC, Rosenberg SA. PD-1 identifies the patient-specific CD8(+) tumor-reactive repertoire infiltrating human tumors. The Journal of clinical investigation. 2014; 124:2246–2259. [PubMed: 24667641]
38. Chen L, Flies DB. Molecular mechanisms of T cell co-stimulation and co-inhibition. Nature reviews. Immunology. 2013; 13:227–242.
39. Yokosuka T, Takamatsu M, Kobayashi-Imanishi W, Hashimoto-Tane A, Azuma M, Saito T. Programmed cell death 1 forms negative costimulatory microclusters that directly inhibit T cell receptor signaling by recruiting phosphatase SHP2. The Journal of experimental medicine. 2012; 209:1201–1217. [PubMed: 22641383]
40. Wherry EJ, Ha SJ, Kaech SM, Haining WN, Sarkar S, Kalia V, Subramaniam S, Blattman JN, Barber DL, Ahmed R. Molecular signature of CD8+ T cell exhaustion during chronic viral infection. Immunity. 2007; 27:670–684. [PubMed: 17950003]
41. Schwartz RH. T cell anergy. Annu Rev Immunol. 2003; 21:305–334. [PubMed: 12471050]
42. Schietinger A, Delrow JJ, Basom RS, Blattman JN, Greenberg PD. Rescued tolerant CD8 T cells are preprogrammed to reestablish the tolerant state. Science. 2012; 335:723–727. [PubMed: 22267581]
43. Schietinger A, Greenberg PD. Tolerance and exhaustion: defining mechanisms of T cell dysfunction. Trends in immunology. 2014; 35:51–60. [PubMed: 24210163]

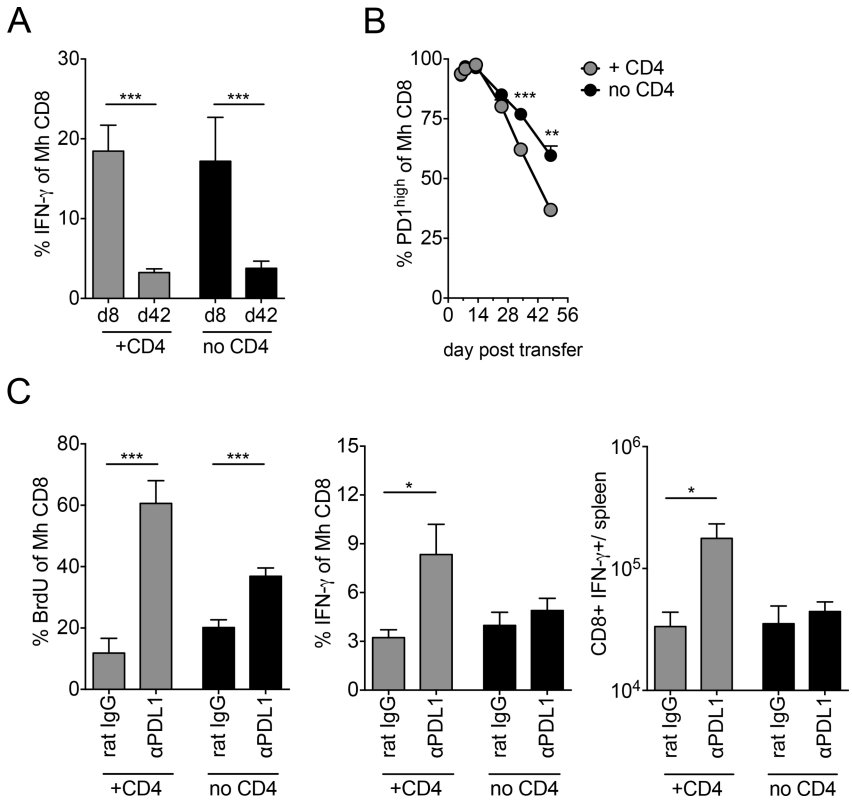

Figure 1. The effect of CD4$^+$ T cell help upon the development of CD8$^+$ T cell exhaustion

1×10^6 CD45.1+ Mh transgenic CD8$^+$ T cells were transferred with or without 2.5×10^6 female B6 CD4$^+$ T cells, 1 week after lethal irradiation of B6 male mice and reconstitution with female B6 BM. *A)* Graph shows mean percentage ± SEM of Mh CD8$^+$ T cells that produced IFN-γ in response to UTY peptide on day 8 and 42 after T cell transfer. Data are pooled from 2 independent experiments (helped n=5-6/group; unhelped n=3-12/group). *B)* Graph showing mean percentage ± SEM of PD-1^{high} Mh CD8+ T cells (n=5/group). *C)* Irradiated male recipients were given 200ug anti-PD-L1 blocking antibody on day 36 and 39 following T cell transfer (n=5 +CD4, n=6 no CD4) or isotype control (n=6 +CD4, n=7 no CD4) before analysis on day 42. From left to right, graphs show mean percentage ± SEM of Mh CD8$^+$ T cells that had incorporated BrdU, mean percentage ± SEM of Mh CD8$^+$ T cells that produced IFN-γ and mean ± SEM absolute numbers of Mh CD8$^+$IFN-γ+ cells/spleen. Data are pooled from 2 independent experiments. Statistical comparisons performed using two-tailed, unpaired student *t*-test: *p<0.05, **p<0.01, ***p<0.001.

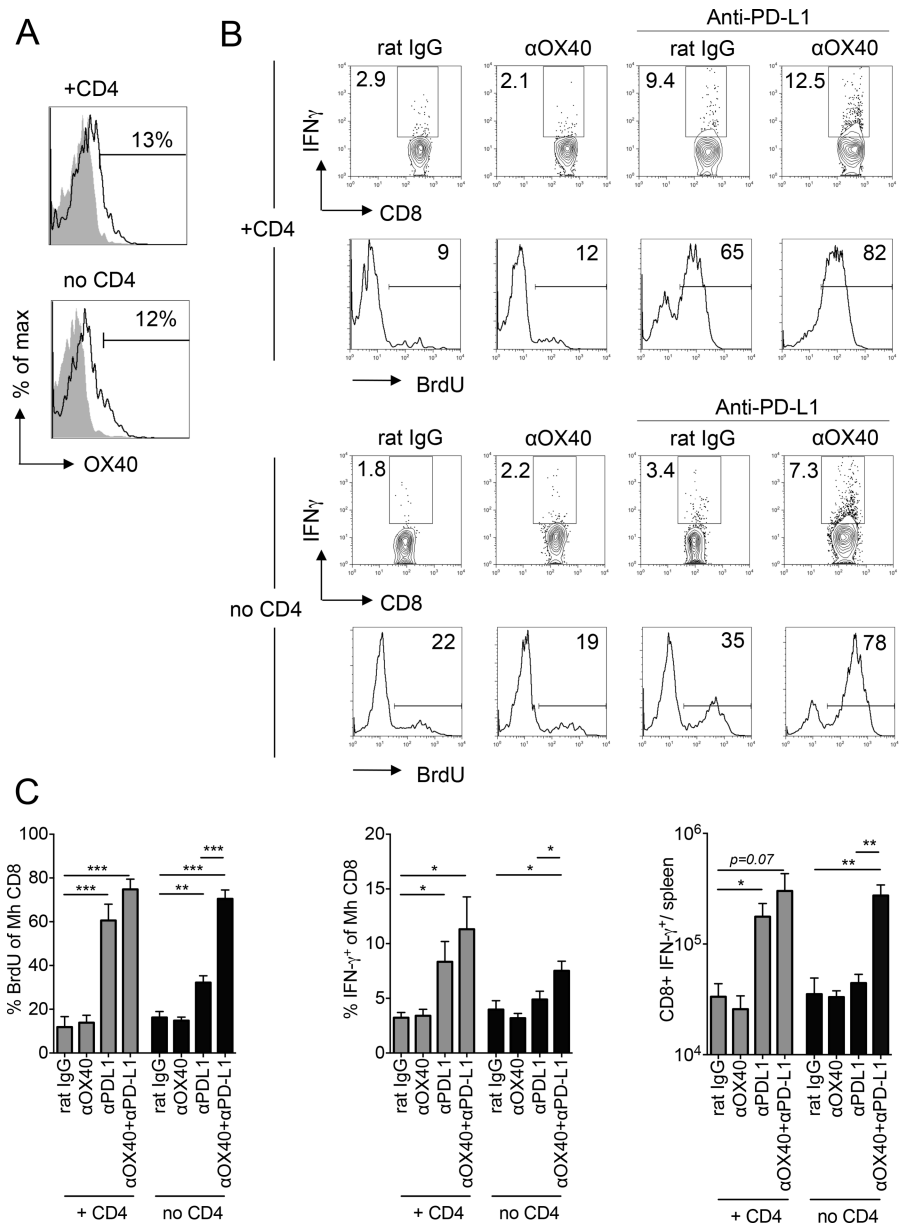

Figure 2. Effect of agonistic anti-OX40 and/or blocking anti-PD-L1 antibody upon helped or unhelped donor Mh CD8$^+$ T cell effector functions

A) Representative histograms showing OX40 expression upon gated Mh CD8$^+$ T cells (open histograms) in recipient spleens on day 42 following transfer to irradiated B6 male mice (mean % OX40+ was 10.5 ±2.2 in helped vs. 11.4 ±2.4 in unhelped; naïve 1.5 ±0.5). Filled histograms show OX40 staining of endogenous cells in same host. *B)* Male BMT recipients were given anti-OX40 i.p. day 35 following Mh CD8$^+$ T cell transfer (with or without CD4$^+$ T cells, n=4/group) or 200ug anti-PD-L1 blocking antibody i.p. day 36 and 39 (n=5 in CD4$^+$, n=6 in no CD4$^+$) or both antibodies (n=6 in + CD4$^+$, and n=7 in no CD4$^+$). Control mice received the same number of i.p. injections with the relevant isotype control (n=6-7). *Top two rows*- representative contour plots show IFN-γ production by helped Mh CD8$^+$ T cells following exposure to UTY peptide, with gates set according to irrelevant peptide and

representative histograms showing the percentage of Mh $CD8^+$ T cells incorporating BrdU. *Bottom two rows* –representative contour plots for IFN-γ production and BrdU incorporation following transfer of unhelped Mh $CD8^+$ T cells. *C)* From left to right, graphs show mean percentage ± SEM of Mh $CD8^+$ T cells that had incorporated BrdU, mean percentage ± SEM of Mh $CD8^+$ T cells that produced IFN-γ and mean ± SEM absolute numbers of Mh $CD8^+$IFN-γ+ cells/spleen. Data are pooled from 2 independent experiments. Statistical comparisons performed using two-tailed, unpaired student *t*-test: *p<0.05, **p<0.01, ***p<0.001.

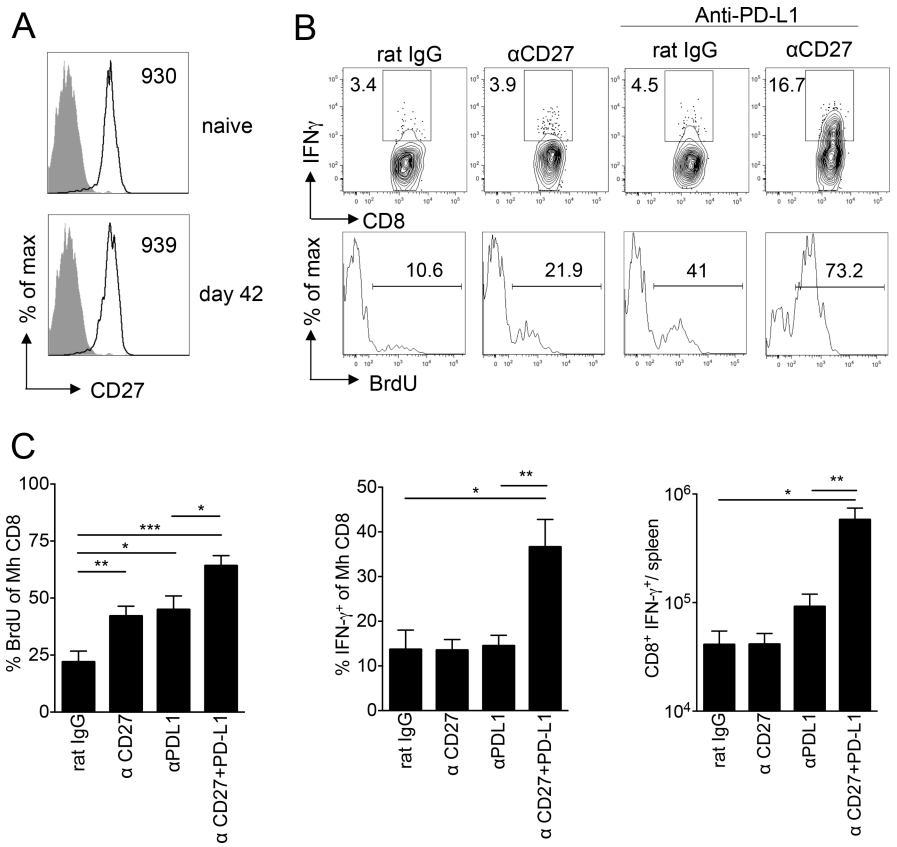

Figure 3. Effect of agonistic anti-CD27 and/or blocking anti-PD-L1 antibody upon unhelped Mh CD8$^+$ T cell effector functions

A) From experiments of similar design to those in Figure 2, representative histograms showing CD27 expression upon naïve input Mh CD8$^+$ T cells or on day 42 (open histograms) following transfer to irradiated male mice and isolation from recipient spleens. Filled histograms show isotype control staining. Numbers indicate mean fluorescence intensity. *B)* BMT recipients were given anti-CD27 on day 35 following unhelped Mh CD8$^+$ T cell transfer (n=8) or 200ug anti-PD-L1 blocking antibody on day 36 and 39 (n=9) or both antibodies (n=9). Control mice received the same number of i.p. injections with the relevant isotype control (n=7). *Top*-representative contour plots show IFN-γ production by Mh CD8$^+$ T cells following exposure overnight to UTY peptide, with gates set according to irrelevant peptide. *Bottom*- representative histograms showing the percentage of Mh CD8$^+$ T cells incorporating BrdU. *C)* Graphs show mean percentage ± SEM of Mh CD8$^+$ T cells that had incorporated BrdU, mean percentage ± SEM of Mh CD8$^+$ T cells that produced IFN-γ and mean ± SEM absolute numbers of Mh CD8$^+$IFN-γ+ cells/spleen. Data are pooled from 2 independent experiments. Statistical comparisons performed using two-tailed, unpaired student *t*-test: *p<0.05, **p<0.01, ***p<0.001.

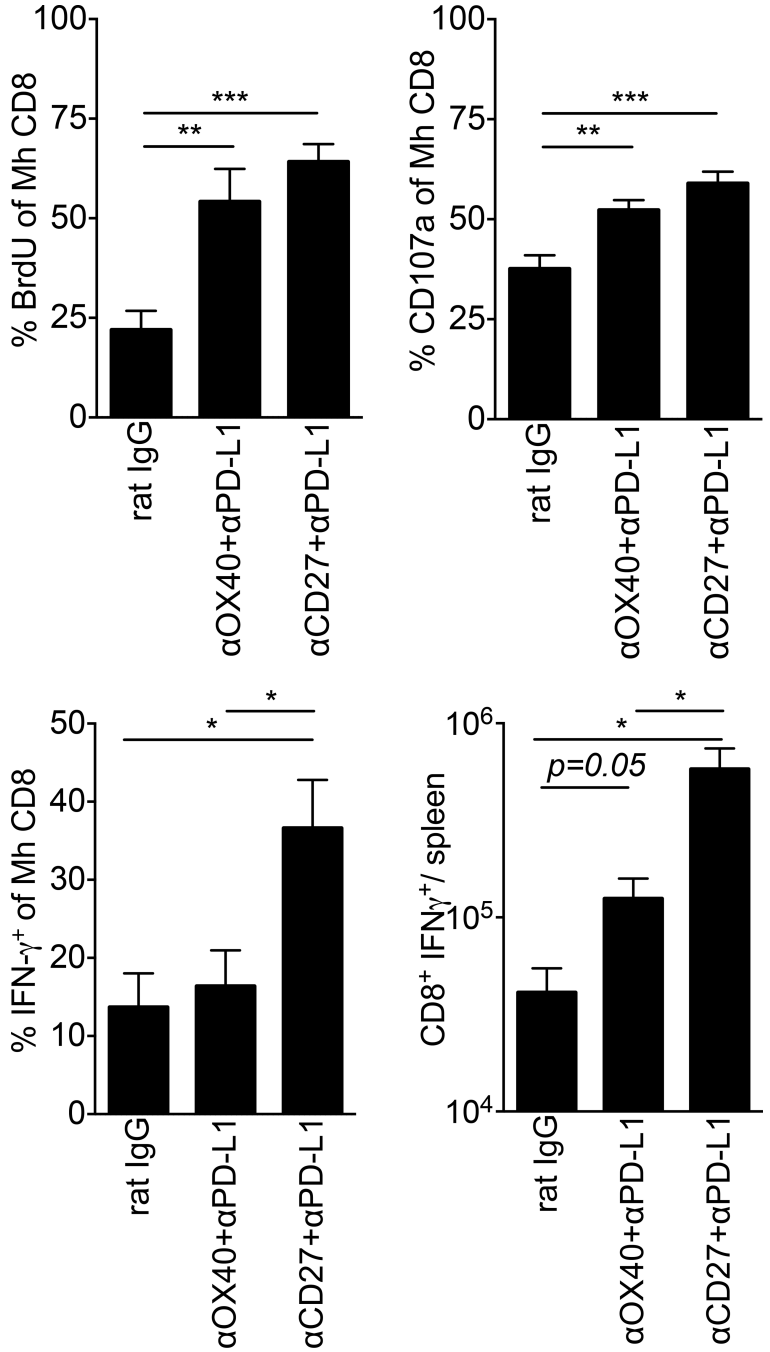

Figure 4. Comparison of agonistic anti-CD27 and anti-OX40 in combination with anti-PD-L1 antibody upon unhelped Mh CD8$^+$ T cell effector functions

Experimental design as set out in Figures 2 and 3. Graphs show mean percentage ± SEM of Mh CD8$^+$ T cells that had incorporated BrdU, mean percentage ± SEM of Mh CD8$^+$ T cells that expressed surface CD107a or intracellular IFN-γ upon restimulation, and mean ± SEM absolute numbers of Mh CD8$^+$IFN-γ+ cells/spleen. Data are pooled from 2 independent experiments (n=7-9/group). Statistical comparisons performed using two-tailed, unpaired student *t*-test: *p<0.05, **p<0.01, ***p<0.001.

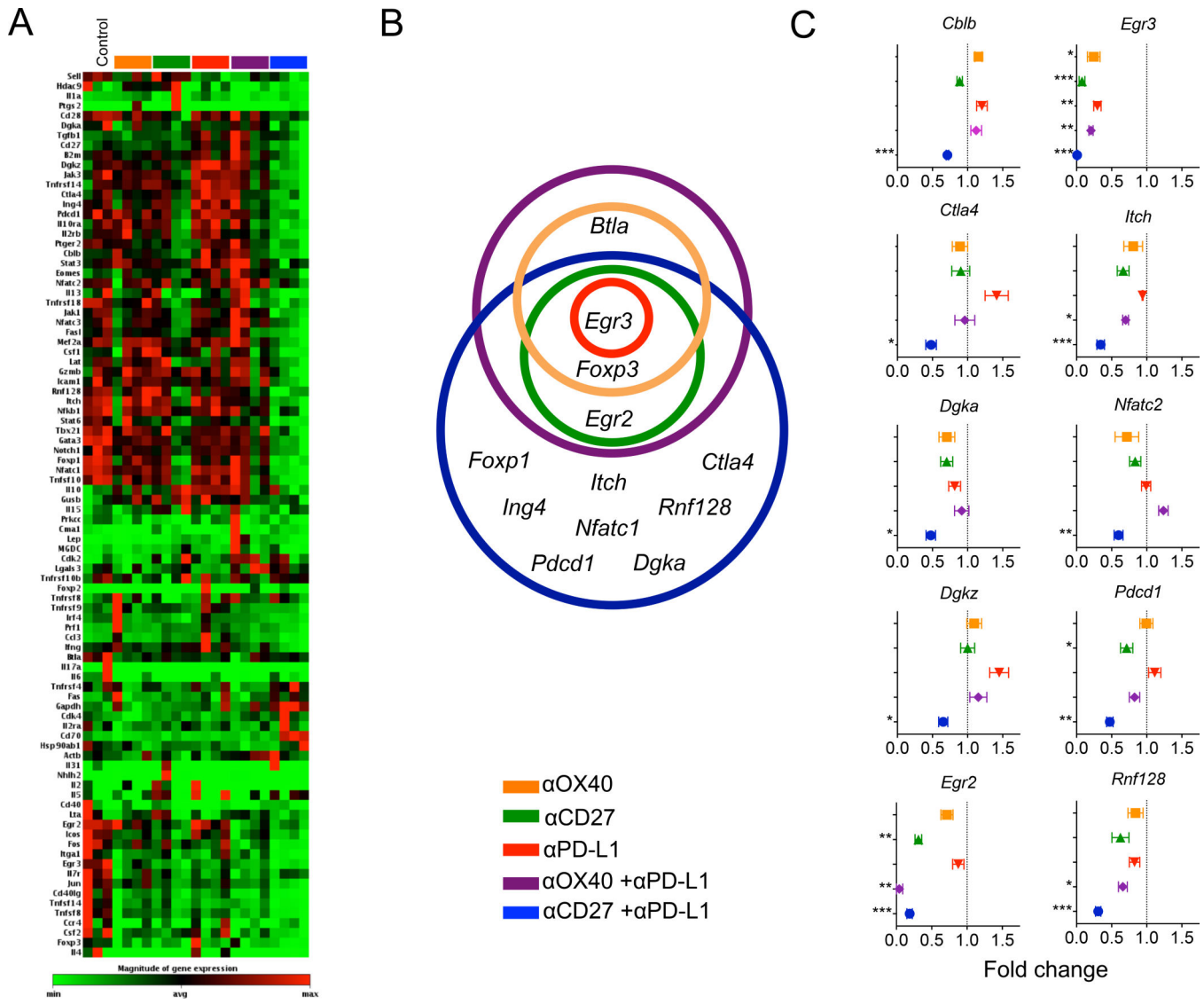

Figure 5. Effect of anti-OX40 and anti-CD27 alone or in combination with anti-PD-L1 upon expression of genes linked to tolerance or effector function

Experimental design as set out in Figures 2-4. On day 42, unhelped Mh $CD8^+$ T cells were flow sorted to high purity from recipient spleens and mRNA extracted (n=3 mice in controls, n=4 mice/group in antibody treatment groups). *A)* Heat map showing quantitative RT-PCR for 84 genes tested (see Materials and Methods). Color code for each group shown within Figure. *B)* Venn diagram showing pattern for >2.0 fold reduction in anergy/quiescence genes according to treatment group. *C)* Graphs showing fold change expression compared to controls for a panel of 10 anergy-quiescence-related genes. The p values were calculated based on an unpaired *t*-test of the replicate $2^{(-\text{delta Ct})}$ values for each gene in the control group and treatment groups: *p<0.05, **p<0.01, ***p<0.001.

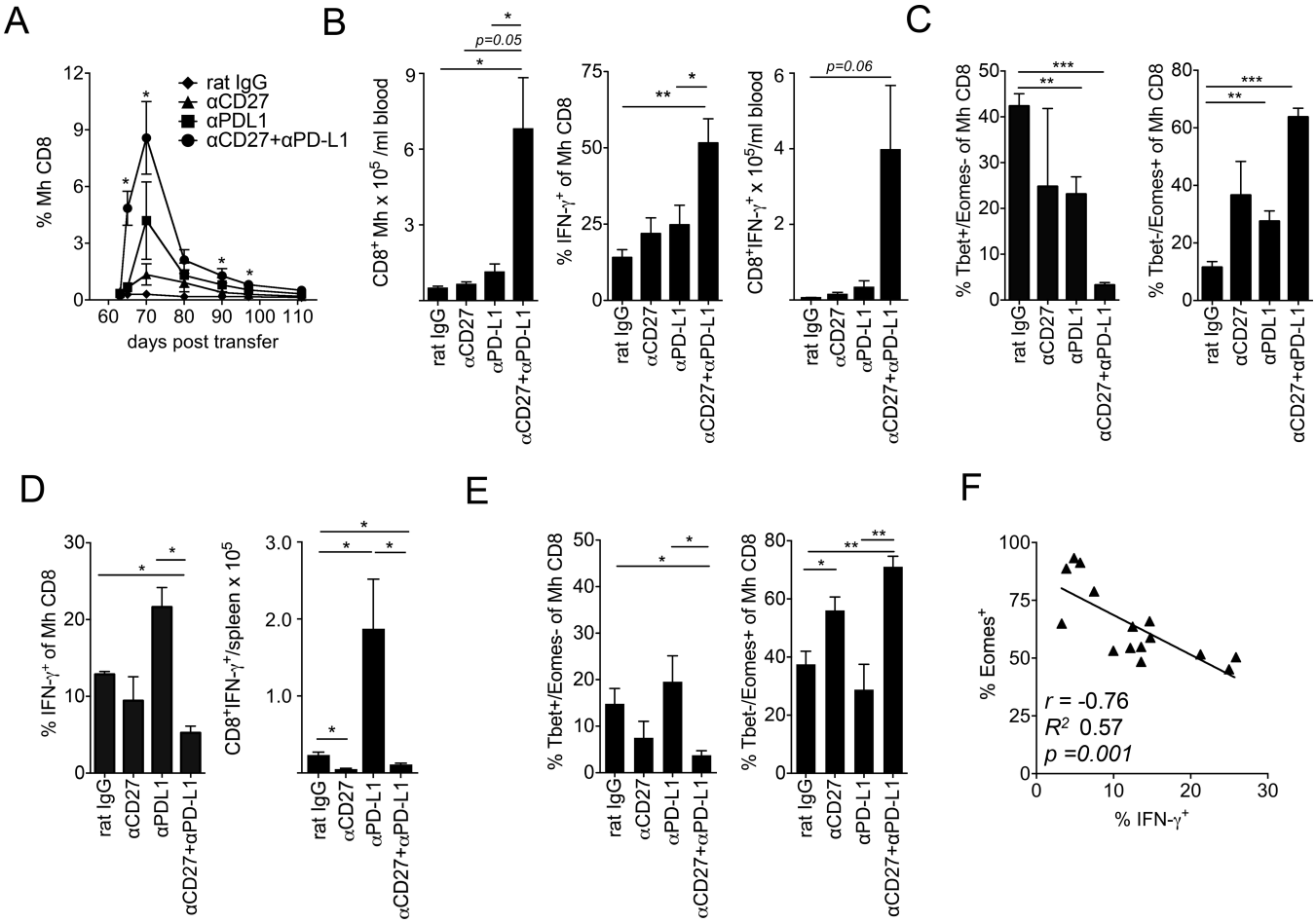

Figure 6. Effect of agonistic anti-CD27 with or without anti-PD-L1 antibody upon unhelped Mh CD8$^+$ T cell T-box factor expression and long term effector functions

Experimental design as set out in Figure 3 except that anti-CD27 was given on day 59 and anti-PD-L1 on day 59 and day 62, with isotype control antibodies given on the same days (n=4/group). *A)* Frequency of blood Mh CD8$^+$ T cells (as % of live gate) following indicated antibody treatment. Statistical comparisons are for combined treatment group versus isotype control. *B-C)* Analyses performed on day 65 in peripheral blood. *B) Left*- Mean ± SEM absolute number of blood Mh CD8$^+$ T cells. *Middle*- Mean percentage ± SEM of blood Mh CD8$^+$ T cells that produced IFN-γ. *Right*- Mean ± SEM absolute number of Mh CD8$^+$IFN-γ + cells/ml blood. *C)* Graphs showing mean % of blood Mh CD8$^+$ T cells that were T-bet^{high}Eomes^{low} (*left*) or T-bet^{low}Eomes^{high} (*right*) on day 65 following transfer. *D-F)* Analyses performed on day 120 in spleen. *D)* Mean percentage ± SEM of Mh CD8$^+$ T cells that produced IFN-γ (*left*) and mean ± SEM absolute numbers of Mh CD8$^+$IFN-γ+ cells/ spleen (*right*) at day 120 following transfer. *E)* Graphs showing mean % of spleen Mh CD8$^+$ T cells that were T-bet^{high}Eomes^{low} (*left*) or T-bet^{low}Eomes^{high} (*right*) on day 120 following transfer. *F)* Scatter plot showing correlation between frequency of IFN-γ+ Mh CD8+ T cells (x-axis) versus frequency of cells that were Eomes+ (y-axis). Data are representative of two

independent experiments with similar design. Statistical comparisons performed using two-tailed, unpaired student *t*-test: *p<0.05, **p<0.01, ***p<0.001.